# UC San Diego
## UC San Diego Previously Published Works

**Title**
Neuronal activity regulates neurotransmitter switching in the adult brain following light-induced stress.

**Permalink**
https://escholarship.org/uc/item/5038k45q

**Journal**
Proceedings of the National Academy of Sciences of the United States of America, 115(20)

**ISSN**
0027-8424

**Authors**
Meng, Da
Li, Hui-Quan
Deisseroth, Karl
et al.

**Publication Date**
2018-05-01

**DOI**
10.1073/pnas.1801598115

Peer reviewed

# Neuronal activity regulates neurotransmitter switching in the adult brain following light-induced stress

Da Meng[a,b,1], Hui-quan Li[a,b], Karl Deisseroth[c,d,e], Stefan Leutgeb[a,b], and Nicholas C. Spitzer[a,b,1]

[a]Neurobiology Section, Division of Biological Sciences and Center for Neural Circuits and Behavior, University of California, San Diego, La Jolla, CA 92093-0357; [b]Kavli Institute for Brain and Mind, University of California, San Diego, La Jolla, CA 92093-0357; [c]Department of Bioengineering, Stanford University, Stanford, CA 94305; [d]Department of Psychiatry and Behavioral Sciences, Stanford University, Stanford, CA 94305; and [e]Howard Hughes Medical Institute, Stanford University, Stanford, CA 94305

Neurotransmitter switching in the adult mammalian brain occurs following photoperiod-induced stress, but the mechanism of regulation is unknown. Here, we demonstrate that elevated activity of dopaminergic neurons in the paraventricular nucleus of the hypothalamus (PaVN) in the adult rat is required for the loss of dopamine expression after long-day photoperiod exposure. The transmitter switch occurs exclusively in PaVN dopaminergic neurons that coexpress vesicular glutamate transporter 2 (VGLUT2), is accompanied by a loss of dopamine type 2 receptors (D2Rs) on corticotrophin-releasing factor (CRF) neurons, and can lead to increased release of CRF. Suppressing activity of all PaVN glutamatergic neurons decreases the number of inhibitory PaVN dopaminergic neurons, indicating homeostatic regulation of transmitter expression in the PaVN.

transmitter switching | stress response | paraventricular nucleus of the hypothalamus | dopaminergic neurons | transmitter coexpression

Activity-dependent neuroplasticity is involved in stress-related disorders in the mature nervous system (1). Activation of the hypothalamic-pituitary-adrenal (HPA) axis by corticotrophin-releasing factor (CRF) is a common stress response pathway.

The paraventricular nucleus of the hypothalamus (PaVN) integrates stress-relevant signals and regulates CRF release through several classic neuroplasticity-related mechanisms. These include changing the amount of glutamate released on CRF neurons after a single action potential and regulating the number of glutamatergic synapses on CRF neurons (2). Additionally, neurotransmitter switching in the PaVN regulates the light-induced stress response (3). Exposing adult rats to a long-day photoperiod [19 h continuous light and 5 h continuous dark per day (19L:5D)] decreases the number of dopaminergic neurons and increases the number of somatostatin neurons in the PaVN compared with the numbers following exposure to a balanced-day photoperiod (12L:12D). This transmitter switch leads to an elevated CRF level in the plasma and to anxious and depressive behaviors. However, the mechanisms by which the release of CRF is regulated by transmitter switching are unclear.

Neuronal activity has been shown to play an essential role in neurotransmitter switching in the developing nervous system: $Ca^{2+}$ spikes regulate transmitter respecification of glutamate and GABA non–cell-autonomously by the release of BDNF in the developing *Xenopus* spinal cord (4–7). Additionally, the ventrolateral suprachiasmatic nucleus (SCN) receives retinal projections from the direct retinohypothalamic tract and indirect geniculohypothalamic tract and entrains internal circadian oscillation to the external light/dark cycle (8–10). These photic signals induce rhythmic c-Fos expression in the SCN (11–13). The PaVN receives direct input from light-sensitive SCN neurons (14–17).

Here, we determined the role of neuronal activity in the regulation of stress-dependent release of CRF in the adult rat, investigating long-day photoperiod-induced transmitter switching in the PaVN.

## Results

### Activity Blockade in PaVN Dopaminergic Neurons Prevents Their Transmitter Switch.

We investigated the change in PaVN neuronal activity in response to long-day photoperiod exposure, using c-Fos as a marker for neuronal activation (18). A 77% increase in the number of c-Fos$^+$ cells was observed in the PaVN after 4 d, but not after 2 d or 2 wk, of long-day photoperiod exposure (19L:5D), compared with balanced-day photoperiod exposure (12L:12D) (Fig. 1 *A* and *B*). The results identify a period of elevation of PaVN neuronal activity. Examining coexpression of c-Fos and tyrosine hydroxylase (TH), a marker for dopaminergic neurons, we found a 63% increase in the number of neurons expressing both TH and c-Fos after 4 d of 19L:5D compared with 12L:12D (Fig. 1 *A* and *C*), indicating increased activity of PaVN dopaminergic neurons. Neurotransmitter switching in the PaVN and subsequent behavioral changes were detected previously only after 1 or 2 wk of altered photoperiod exposure (3). Therefore, elevation in overall PaVN neuronal activity and the activity of PaVN dopaminergic neurons occurs before the detection of transmitter switching.

To investigate the role of elevated PaVN neuronal activity in regulating transmitter switching that can control the subsequent stress response, we suppressed the activity of PaVN dopaminergic

---

**Significance**

The discovery that neurotransmitter identity is regulated by activity in the adult mammalian brain during a stress response raises questions about the extent and function of this plasticity. Specific synapses are associated with the release of a particular neurotransmitter or transmitters on the basis of evidence obtained under a single set of conditions. Transmitter switching endows the connectome with greater plasticity: Activity-dependent revision of signaling provides another dimension of flexibility to regulate normal behavior. Changes in transmitter identity are also positioned to contribute to diseases of the nervous system. Neurotransmitter imbalance has long been implicated in common neurological and psychiatric disorders, provoking interest in transmitter switching as a therapeutic tool for patients.
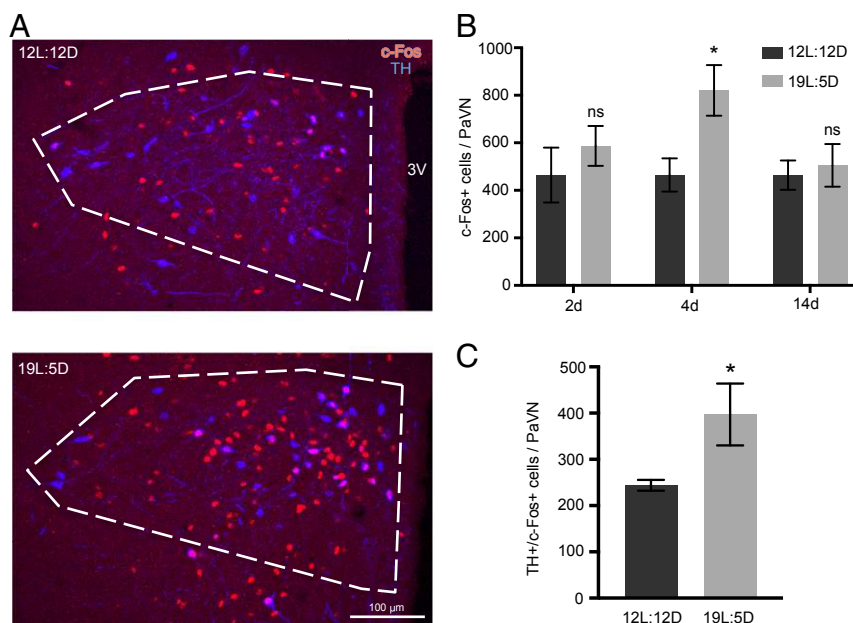
---

**Fig. 1.** Activity of PaVN neurons is elevated after long-day photoperiod exposure. WT rats were exposed to either a long-day photoperiod (19L:5D) or balanced-day photoperiod (12L:12D) for 2, 4, or 14 d. Immunofluorescent staining of TH and c-Fos was performed with fixed brain sections. (*A*) Confocal images of the PaVN after 4 d of exposure; white dashed lines indicate the PaVN boundary. 3V, third ventricle. (*B*) Quantification of the number of c-Fos$^+$ cells in the PaVN per animal after different durations of exposure: 12L:12D for 2 d, $n = 4$ animals; 19L:5D for 2 d, $n = 4$ animals; 12L:12D for 4 d, $n = 6$ animals; 19L:5D for 4 d, $n = 6$ animals; 12L:12D for 14 d, $n = 4$ animals; and 19L:5D, $n = 5$ animals. Welch's $t$ test (2 d, $P = 0.4267$; 4 d, $P = 0.0216$; 14 d, $P = 0.7209$). Data are mean ± SEM. *$P < 0.05$. ns, not significant. (*C*) Quantification of the number of TH$^+$/c-Fos$^+$ cells in the PaVN per animal after 4 d of exposure to 12L:12D or 19L:5D ($n = 6$ animals per condition). Welch's $t$ test ($P = 0.0478$). Data are mean ± SEM. *$P < 0.05$.

neurons specifically using TH-Cre transgenic rats stereotaxically injected with a Cre-dependent adeno-associated virus (AAV)-double-floxed inverse open reading frame (DIO)-inwardly rectifying potassium channel (Kir). This TH-Cre rat line has been used successfully in studies of ventral tegmental area (VTA) dopamine neuron function and transmitter coexpression (19, 20). By hyperpolarizing transfected neurons, Kir has been shown to inhibit action potentials and elevations of intracellular Ca$^{2+}$ (5, 21). AAV-DIO-EYFP was used as a control. To allow sufficient viral expression, 4 wk after injection rats were exposed to either 19L:5D or 12L:12D for 2 wk. Kir expression indeed suppressed activity of PaVN dopaminergic neurons examined by c-Fos expression (*SI Appendix*, Fig. S1*C*). There was no difference in the number of TH$^+$ neurons between the Kir and EYFP groups after 12L:12D (Fig. 2), indicating that suppressing the activity of PaVN dopaminergic neurons has no effect on their TH expression in response to the balanced-day photoperiod. However, after a 2-wk exposure to 19L:5D, there was a marked decrease in the number of TH$^+$ neurons in the control EYFP group (Fig. 2), consistent with previous results (3). No significant apoptosis was detected in EYFP-expressing rats exposed to either 12L:12D or 19L:5D, indicating the decrease in dopaminergic neurons was not associated with cell death (*SI Appendix*, Fig. S1 *A and B*). This decrease in the number of TH$^+$ neurons was abolished in the Kir group following 19L:5D exposure. Blocking elevated activity of PaVN dopaminergic neurons resulted in significantly more TH$^+$ neurons after long-day exposure compared with the EYFP control; the number of TH$^+$ neurons was no longer significantly different from the number following balanced-day exposure (Fig. 2). This result suggests that suppressing electrical activity of PaVN dopaminergic neurons is sufficient to block their transmitter switch elicited by exposure to the long-day photoperiod.

**Switchable PaVN Dopaminergic Neurons Coexpress the Vesicular Glutamate Transporter 2.** Neurotransmitter coexpression and corelease have been reported in many areas of the adult mammalian brain (20, 22–25). Previous studies of neurotransmitter expression patterns in the PaVN have revealed coexpression of a myriad of neuropeptides (26). However, transmitter coexpression of dopamine with classical neurotransmitters, such as glutamate, has yet to be examined in the PaVN. Vesicular glutamate transporter 2 (VGLUT2) is the dominant form of synaptic vesicle transporter for glutamatergic neurons in the hypothalamus and midbrain (27, 28).

We performed immunostaining of TH and VGLUT2 to examine the colocalization of the two proteins in the same cell bodies in the PaVN of rats maintained on the 12L:12D photoperiod (Fig. 3*A*). At the protein level, $49.0 ± 2.7\%$ of PaVN dopaminergic neurons coexpressed VGLUT2 (1,170 of 2,379 neurons from four animals). However, TH$^+$/VGLUT2$^+$ neurons constitute only $9.9 ± 0.6\%$ of all neurons expressing VGLUT2 (397 of 4,197 neurons from three animals). At the RNA level, we used RNAscope, a highly sensitive fluorescent in situ hybridization method capable of detecting individual RNA molecules, to examine the co-occurrence of TH mRNA and VGLUT2 mRNA puncta in the same cell bodies in the PaVN. TH immunostaining was performed with RNAscope to reliably identify cell boundaries of dopaminergic neurons (Fig. 3*B*). A total of $47.7 ± 2.6\%$ of TH protein$^+$ cell bodies contained both TH mRNA and VGLUT2 mRNA puncta in the PaVN (280 of 582 neurons from three animals), indicating significant coexpression of TH and VGLUT2 at the mRNA level as well. The activity of PaVN VGLUT2$^+$ neurons increased significantly after 4 d of 19L:5D exposure, but the number of VGLUT2$^+$ neurons in the PaVN remained unchanged after 2 wk of exposure to 19L:5D (*SI Appendix*, Fig. S2 *A–C*).

We hypothesized that these two subpopulations of PaVN dopaminergic neurons, VGLUT2$^+$ versus VGLUT2$^-$, decrease their expression of TH to different extents after 19L:5D exposure. To test this hypothesis, we counted the number of neurons expressing both TH and VGLUT2 (TH$^+$VGLUT2$^+$) and the number of neurons expressing only TH (TH$^+$VGLUT2$^-$) in the PaVN after 2 wk of exposure to 19L:5D or 12L:12D. Interestingly,
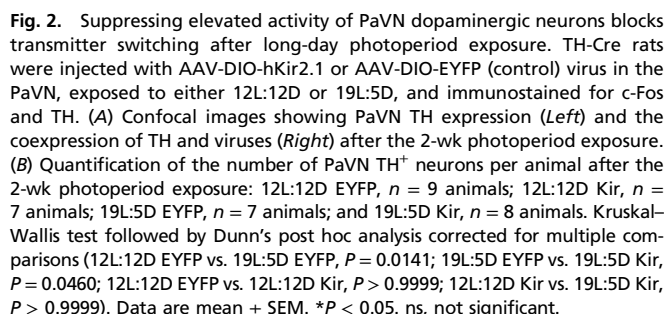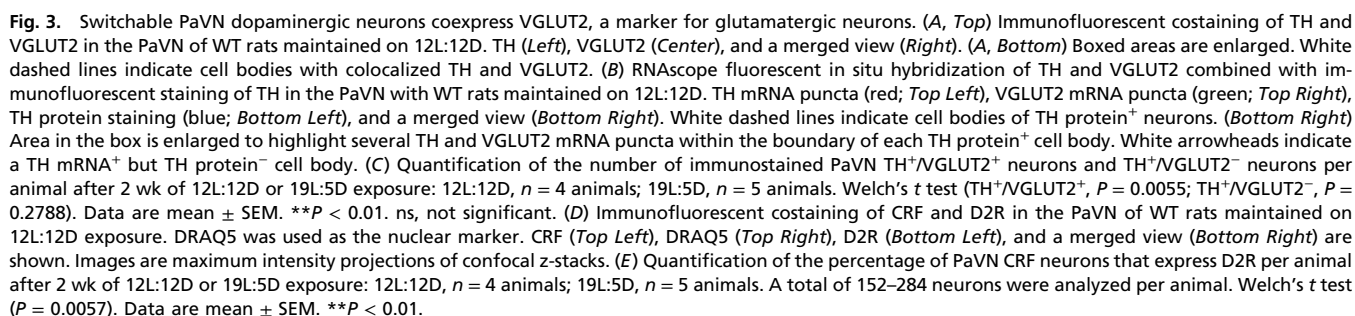
**Fig. 2.** Suppressing elevated activity of PaVN dopaminergic neurons blocks transmitter switching after long-day photoperiod exposure. TH-Cre rats were injected with AAV-DIO-hKir2.1 or AAV-DIO-EYFP (control) virus in the PaVN, exposed to either 12L:12D or 19L:5D, and immunostained for c-Fos and TH. (*A*) Confocal images showing PaVN TH expression (*Left*) and the coexpression of TH and viruses (*Right*) after the 2-wk photoperiod exposure. (*B*) Quantification of the number of PaVN TH$^+$ neurons per animal after the 2-wk photoperiod exposure: 12L:12D EYFP, $n$ = 9 animals; 12L:12D Kir, $n$ = 7 animals; 19L:5D EYFP, $n$ = 7 animals; and 19L:5D Kir, $n$ = 8 animals. Kruskal–Wallis test followed by Dunn's post hoc analysis corrected for multiple comparisons (12L:12D EYFP vs. 19L:5D EYFP, $P$ = 0.0141; 19L:5D EYFP vs. 19L:5D Kir, $P$ = 0.0460; 12L:12D EYFP vs. 12L:12D Kir, $P$ > 0.9999; 12L:12D Kir vs. 19L:5D Kir, $P$ > 0.9999). Data are mean ± SEM. *$P$ < 0.05. ns, not significant.

only TH$^+$VGLUT2$^+$ neurons decreased significantly in number after 19L:5D, by 35.0% (Fig. 3*C*). This result demonstrates that the neurotransmitter switch of PaVN dopaminergic neurons occurs only in the subpopulation that coexpresses VGLUT2.

An elevated blood plasma cortisol level, indicating an activated HPA axis, is associated with the stress response induced by exposure to the 19L:5D photoperiod (3). PaVN CRF neurons express excitatory glutamate receptors, and glutamate stimulates CRF release (2, 29). Since we observed significant overlap between the PaVN glutamatergic and dopaminergic neuronal populations, we investigated whether PaVN CRF neurons also receive inhibitory dopaminergic input by immunostaining of CRF and dopamine type 2 receptor (D2R), an inhibitory dopamine receptor. Indeed, at the baseline level, 43.7 ± 2.0% of PaVN CRF neurons expressed D2R. After 2 wk of 19L:5D exposure, the percentage of CRF neurons expressing D2R decreased to 26.6 ± 3.6% (Fig. 3 *D* and *E* and *SI Appendix*, Fig. S2 *D* and *E*).

Collectively, these results suggest a mechanism by which the decreased number of PaVN dopamine- and glutamate-coexpressing neurons after 19L:5D exposure leads to the stress response. The excitatory synaptic input to CRF neurons remains the same, while the expression levels of both presynaptic dopamine and inhibitory postsynaptic D2R decrease, leading to increased activity of postsynaptic CRF neurons and subsequent activation of the HPA axis.

**Homeostatic Decrease of PaVN Inhibitory Dopaminergic Neurons Following Activity Blockade of PaVN Excitatory Glutamatergic Neurons.** Activity-dependent transmitter switching in the developing nervous system is often compensatory and homeostatic (6, 30). Accordingly, we investigated whether manipulating the neuronal activity of PaVN excitatory glutamatergic neurons changes the number of inhibitory dopaminergic neurons in the adult rat brain. To suppress the activity of PaVN glutamatergic neurons, AAV-DIO-Kir was injected, together with a Cre-expressing AAV virus driven by the CaMKII promoter (AAV-CaMKII-Cre) that has been commonly used to target excitatory glutamatergic neurons (31). AAV-DIO-Kir was replaced with AAV-DIO-EYFP in the control group. Animals were maintained on a 12L:12D light/dark cycle throughout the experiment. The viral infection profile reflects the coexpression profile of dopamine and glutamate in PaVN neurons noted above (8.9 ± 1.3% of all virus$^+$ neurons are also TH$^+$, 811 neurons from three animals; 46.7 ± 11.0% of all TH$^+$ neurons are also virus$^+$, 522 neurons from three animals). Kir expression in glutamatergic neurons effectively reduced neuronal activity in the PaVN, as indicated by a 49% decrease in the number of PaVN c-Fos$^+$ cells (*SI Appendix*, Fig. S3 *A* and *B*). We observed a significant decrease in the number of PaVN TH$^+$ neurons in the CaMKII-Kir group compared with the control (Fig. 4 *A* and *B*), indicating that suppressing the activity of PaVN excitatory neurons decreases the number of PaVN inhibitory dopaminergic neurons. Cell death is unlikely to have contributed to the decreased number of dopaminergic neurons since the total number of neurons, neuronal density, and percentage of apoptotic cells in the PaVN remained unchanged between the CaMKII-Kir and CaMKII-EYFP groups (*SI Appendix*, Fig. S3 *C–G*).

To test the specificity of the homeostatic decrease in PaVN dopaminergic neurons, we investigated whether suppressing the activity of glutamatergic neurons affects other neurotransmitters in the PaVN. Nitric oxide (NO) is expressed in the PaVN and is differentially expressed in patients and animal models of stress and depressive disorders (32–34). Dopaminergic neurons and neurons expressing neuronal nitric oxide synthase (nNOS), a marker for NO neurons, are intermingled but separate populations in the PaVN. There is no difference in the number of PaVN nNOS$^+$ neurons between the CaMKII-Kir and CaMKII-EYFP groups (Fig. 4 *C* and *D*), suggesting that suppressing the activity of PaVN glutamatergic neurons does not change the number of PaVN NO neurons. Therefore, the observed decrease

**Fig. 3.** Switchable PaVN dopaminergic neurons coexpress VGLUT2, a marker for glutamatergic neurons. (*A*, *Top*) Immunofluorescent costaining of TH and VGLUT2 in the PaVN of WT rats maintained on 12L:12D. TH (*Left*), VGLUT2 (*Center*), and a merged view (*Right*). (*A*, *Bottom*) Boxed areas are enlarged. White dashed lines indicate cell bodies with colocalized TH and VGLUT2. (*B*) RNAscope fluorescent in situ hybridization of TH and VGLUT2 combined with immunofluorescent staining of TH in the PaVN with WT rats maintained on 12L:12D. TH mRNA puncta (red; *Top Left*), VGLUT2 mRNA puncta (green; *Top Right*), TH protein staining (blue; *Bottom Left*), and a merged view (*Bottom Right*). White dashed lines indicate cell bodies of TH protein$^+$ neurons. (*Bottom Right*) Area in the box is enlarged to highlight several TH and VGLUT2 mRNA puncta within the boundary of each TH protein$^+$ cell body. White arrowheads indicate a TH mRNA$^+$ but TH protein$^-$ cell body. (*C*) Quantification of the number of immunostained PaVN TH$^+$/VGLUT2$^+$ neurons and TH$^+$/VGLUT2$^-$ neurons per animal after 2 wk of 12L:12D or 19L:5D exposure: 12L:12D, $n = 4$ animals; 19L:5D, $n = 5$ animals. Welch's $t$ test (TH$^+$/VGLUT2$^+$, $P = 0.0055$; TH$^+$/VGLUT2$^-$, $P = 0.2788$). Data are mean ± SEM. **$P < 0.01$. ns, not significant. (*D*) Immunofluorescent costaining of CRF and D2R in the PaVN of WT rats maintained on 12L:12D exposure. DRAQ5 was used as the nuclear marker. CRF (*Top Left*), DRAQ5 (*Top Right*), D2R (*Bottom Left*), and a merged view (*Bottom Right*) are shown. Images are maximum intensity projections of confocal z-stacks. (*E*) Quantification of the percentage of PaVN CRF neurons that express D2R per animal after 2 wk of 12L:12D or 19L:5D exposure: 12L:12D, $n = 4$ animals; 19L:5D, $n = 5$ animals. A total of 152–284 neurons were analyzed per animal. Welch's $t$ test ($P = 0.0057$). Data are mean ± SEM. **$P < 0.01$.

in the number of PaVN dopaminergic neurons appears to be specific to this neuronal population following activity blockade of PaVN glutamatergic neurons.

We then tested whether the decrease in the number of dopaminergic neurons is caused by decreased neuronal activity of glutamatergic neurons specifically or by a decrease in overall neuronal activity in the PaVN. Global suppression of PaVN neuronal activity was achieved by injecting AAV-DIO-Kir coupled with a Cre-expressing AAV virus driven by the human Synapsin promoter (AAV-Synapsin-Cre) (35). Since the PaVN contains a significant number of GABAergic neurons (36) and peptide-expressing neurons in addition to glutamatergic neurons, Kir was likely expressed in all of these cell types. We observed a 49.9% reduction in the number of c-Fos$^+$ cells in the PaVN of animals maintained on a 12L:12D cycle, comparable to the level of activity blockade achieved by suppressing glutamatergic neurons alone (*SI Appendix*, Fig. S3 *A, B, H,* and *I*). However, there is no difference in the number of TH$^+$ neurons between the Synapsin-Kir and Synapsin-EYFP groups (Fig. 4 *E* and *F*). These results suggest that the decreased number of dopaminergic neurons on a balanced light/dark cycle is caused specifically by suppressing the activity of glutamatergic neurons in the PaVN, further supporting the homeostatic regulation of neurotransmitter switching in the adult nervous system.

## Discussion

### Cell Population-Autonomous Mechanism of Neurotransmitter Switching in the Adult Brain.

Many forms of neuroplasticity are regulated by neuronal activity through either cell-autonomous or non–cell-autonomous mechanisms. On one hand, it is well established that elevated intracellular Ca$^{2+}$ following depolarization serves as a second messenger and can cause transcriptional and translational changes of neurotransmitter synthetic enzymes, receptors, and ion channels of the same neurons (37). On the other hand, cell secretion and cell-to-cell surface signaling can be regulated by neuronal activity and affect intracellular signaling of neighboring neurons non–cell-autonomously. In the developing *Xenopus* spinal cord, the mechanism through which neuronal activity regulates transmitter switching is non–cell-autonomous through secretion of BDNF (5).

Our results indicate that c-Fos activity of both the total PaVN neuronal population and PaVN dopaminergic neurons specifically is elevated briefly during long-day photoperiod exposure. The absence of elevation of c-Fos after 2 d was not surprising because transmitter switching requires sustained activity over a period of days; however, the observation that it has come down at 2 wk was unexpected. Perhaps c-Fos builds up, triggers switching (5, 7), and is then down-regulated in the face of continued stimulation through a separate mechanism yet to be explored. The elevation in neuronal activity occurs before previously detected changes in
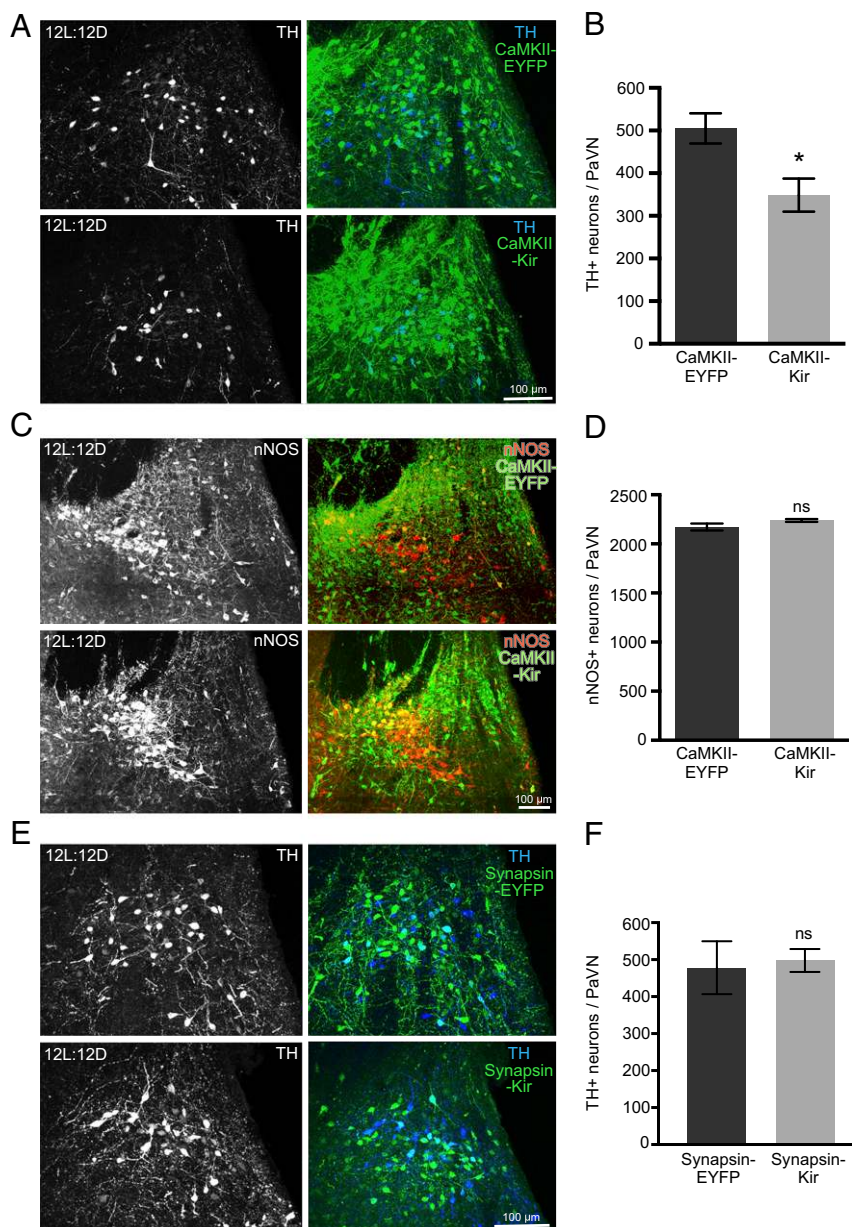
**Fig. 4.** Suppressing activity of PaVN excitatory neurons decreases the number of PaVN dopaminergic neurons after balanced-day photoperiod exposure. (*A*–*D*) WT rats were injected with AAV-CaMKII-Cre together with AAV-DIO-hKir2.1 (CaMKII-Kir) in the PaVN to suppress the activity of glutamatergic neurons. AAV-DIO-hKir2.1 was replaced with AAV-DIO-EYFP (CaMKII-EYFP) in the control group. Animals were maintained on 12L:12D after injection. (*A*) Coexpression of TH and viruses in the PaVN by immunofluorescence. TH (*Left*), a merged view of TH and virus (*Right*), CaMKII-EYFP (*Top*), and CaMKII-Kir (*Bottom*). (*B*) Quantification of the number of PaVN TH$^+$ neurons per animal in the CaMKII-EYFP group versus the CaMKII-Kir group: $n = 6$ animals per condition. Welch's $t$ test ($P = 0.0141$). Data are mean $\pm$ SEM. *$P < 0.05$. (*C*) Coexpression of nNOS and viruses in the PaVN by immunofluorescence. nNOS (*Left*), a merged view of nNOS and virus (*Right*), CaMKII-EYFP (*Top*), and CaMKII-Kir (*Bottom*). (*D*) Quantification of the number of PaVN nNOS$^+$ neurons per animal in the CaMKII-EYFP group versus the CaMKII-Kir group: CaMKII-EYFP, $n = 5$ animals; CaMKII-Kir, $n = 4$ animals. Welch's $t$ test ($P = 0.1420$). Data are mean $\pm$ SEM. ns, not significant. (*E* and *F*) WT rats were injected with AAV-Synapsin-Cre together with AAV-DIO-hKir2.1 (Synapsin-Kir) in the PaVN to suppress the activity of all neurons. AAV-DIO-hKir2.1 was replaced with AAV-DIO-EYFP (Synapsin-EYFP) in the control group. Animals were maintained on 12L:12D after injection. (*E*) Coexpression of TH and viruses in the PaVN by immunofluorescence. TH (*Left*), a merged view of TH and virus (*Right*), Synapsin-EYFP (*Top*), and Synapsin-Kir (*Bottom*). (*F*) Quantification of the number of PaVN TH$^+$ neurons per animal in the Synapsin-EYFP group versus the Synapsin-Kir group: Synapsin-EYFP, $n = 5$ animals; Synapsin-Kir, $n = 10$ animals. Welch's $t$ test ($P = 0.8110$). Data are mean $\pm$ SEM.

neurotransmitter expression or anxiety and depression-like behaviors. Given this temporal sequence of the changes, a long-day photoperiod likely leads to elevated PaVN c-Fos activity through the efferent projections from the retina to the SCN and then to the PaVN, which in turn results in transmitter switching and subsequent changes in behavior (3). We find that suppressing the elevation of PaVN dopaminergic neuronal activity during the

long-day photoperiod blocks the transmitter switch, providing experimental support for this hypothesis.

In the present study, suppressing the activity of the population of dopaminergic neurons by Kir expression in TH-Cre rats was sufficient to block their transmitter switch in response to long-day photoperiod exposure. It would be challenging to test whether manipulating the activity of single dopaminergic neurons changes

their likelihood of switching transmitters after long-day exposure in vivo. Theoretically, sparse infection of dopaminergic neurons by either Kir or control virus, followed by long-day exposure, could address whether manipulating the activity of single dopaminergic neurons causes a transmitter switch. However, with the only currently available rat TH-Cre transgenic line targeting dopaminergic neurons, $25.7 \pm 2.2\%$ of PaVN virus-infected neurons do not express a detectable level of TH protein (*SI Appendix*, Fig. S1*D*). This likely reflects the highly plastic and variable nature of TH expression, since we frequently observe clusters of TH mRNA puncta in the PaVN, implying the presence of neuron cell bodies that are TH mRNA$^+$ but TH protein$^-$ (Fig. 3*B*). The "ectopic" expression in a TH-Cre mouse line has been attributed to sufficient Cre expression in weakly TH mRNA or protein-expressing neurons (38). The moderate decrease in the number of TH protein$^+$ neurons after long-day photoperiod exposure, the mismatch between the "on or off" nature of the Cre-medicated recombination event, and the variable endogenous TH protein expression level in TH-Cre rats would combine to introduce significant variability to the sparse infection approach. We conclude from our assay that transmitter switching in the adult brain is cell population-autonomous; whether it is single cell-autonomous remains to be tested.

**Neurotransmitter Coexpression and Neurotransmitter Switch.** Transmitter switching and transmitter coexpression and corelease may be intrinsically linked biological processes: Neurons that normally coexpress two or more neurotransmitters may up- or down-regulate each individual transmitter differentially in response to external stimuli and give rise to functional neurotransmitter switching (39).

Coexpression of TH and VGLUT2 has been reported in rat VTA and posterior hypothalamus in cell bodies in vitro and in vivo (20, 40–42). Additionally, axons from VTA dopaminergic neurons contain TH, VMAT, and VGLUT2, and they corelease both dopamine and glutamate in the nucleus accumbens (20, 41, 43). Our study demonstrates the coexpression of TH and VGLUT2 in the cell bodies of PaVN dopaminergic neurons both at the mRNA level and at the protein level. We observed a marked decrease in the number of PaVN TH$^+$VGLUT2$^+$ neurons after 19L:5D exposure but no change in the number of TH$^+$VGLUT2$^-$ neurons. Given that the overall number of PaVN VGLUT2$^+$ neurons remains unchanged after 19L:5D exposure, it is likely that neurons expressing both dopamine and glutamate at 12L:12D lose their dopamine expression after 19L:5D but retain their glutamate expression.

It is intriguing that in all known cases of neurotransmitter switching, only a moderate percentage of neurons express a certain neurotransmitter switch, while the others expressing the same transmitter in the same anatomical location do not. It has long been speculated that neurons that switch their transmitter and neurons that appear not to do so belong to different functional subpopulations, but biological markers to distinguish them have been lacking. In the present study, only VGLUT2$^+$ PaVN dopaminergic neurons undergo photoperiod-induced transmitter switching, while VGLUT2$^-$ ones do not, suggesting that coexpression of neurotransmitters might be used to distinguish switchable from nonswitchable neurons and elucidate their potential functional differences. On the other hand, projection patterns and connectivity within local circuits can also be used to classify adjacent neurons expressing the same neurotransmitter into different subgroups. Little is known about the projections and local connectivity of PaVN DA neurons, which need to be explored in future studies.

PaVN CRF neurons are potential targets of PaVN TH$^+$VGLUT2$^+$ neurons to mediate the light-induced stress response since they reside in close proximity and express both ionotropic excitatory glutamate receptors (29) and D2R inhibitory dopamine receptors

(Fig. 3 *D* and *E*). Removal of inhibitory input, in addition to increased glutamate release, seems to be necessary for the activation of PaVN CRF neurons to trigger the stress response (44), although previous studies have largely focused on the role of the inhibitory neurotransmitter GABA. In the present study, down-regulation of presynaptic TH coupled with decreased expression of postsynaptic D2Rs provides a separate mechanism to reduce the inhibitory input to CRF neurons, facilitating the activation of CRF neurons by elevated activity of presynaptic glutamatergic neurons. Elevated CRF release then triggers activation of the HPA axis and contributes to the increased stress and anxiety behaviors observed in rodents following exposure to long-day photoperiods.

**Homeostatic Regulation of the Activity-Dependent Transmitter Switch in the Adult Brain.** Accumulating evidence suggests transmitter switching is regulated homeostatically by neuronal activity; that is, the changes of neurotransmitter phenotypes following a given perturbation often attempt to compensate for the change and retain stable function of the neuronal circuit. For example, suppressing the activity of spinal neurons by removing extracellular calcium or expressing Kir during development increased the number of neurons expressing the excitatory neurotransmitters glutamate and acetylcholine and decreased the number of neurons expressing the inhibitory neurotransmitters GABA and glycine. Enhancing neuronal activity caused the opposite changes (6). Here, we observed that suppressing the neuronal activity of excitatory glutamatergic neurons in the PaVN decreased the number of inhibitory dopaminergic neurons, providing evidence for homeostatic regulation of transmitter switching in the adult brain. It is intriguing that PaVN dopaminergic neurons respond to distinct stimuli by down-regulating their TH expression differently, either after a long-day photoperiod or after silencing of neighboring glutamatergic neurons. This may reflect their diverse roles in the PaVN stress circuitry, where both external environmental stressors and internal stress signals from multiple brain regions are integrated and processed. Homeostatic regulation of the number of dopaminergic PaVN neurons in response to the activity of glutamatergic neurons was not observed following 2 wk of long-day exposure. The absence of homeostatic regulation in this case may be explained by a difference in stimulus strength, if constitutive suppression of activity with Kir is a stronger manipulation of activity than natural light exposure.

**Model of Activity-Dependent Regulation of Transmitter Switching Causing Light-Induced Stress.** We propose a model of activity-dependent transmitter switching in the adult rat PaVN leading to photoperiod-induced stress (Fig. 5). The balanced-day photoperiod stimulates a low level of activity in PaVN glutamatergic and dopaminergic neurons. By expressing both excitatory glutamate receptors and inhibitory dopamine receptors, PaVN CRF neurons also exhibit a low level of activity and a low level of CRF is detected in the bloodstream. After stressful long-day photoperiod exposure, the activity of PaVN glutamatergic and dopaminergic neurons is significantly elevated. This leads to a decrease in the expression of dopamine in the glutamate/dopamine coexpressing neurons, while expression of glutamate is sustained. Coupled with decreased D2R expression on CRF neurons, the increased excitatory and decreased inhibitory inputs to CRF neurons cause substantial CRF release and the subsequent stress response. For simplicity, switching and nonswitching neurons are suggested to target the same CRF cells; whether or not this is the case will be the subject of future work. On the other hand, when the activity of PaVN glutamatergic neurons is artificially suppressed during the balanced-day photoperiod, PaVN dopamine expression decreases to maintain the homeostatic regulation of CRF neuronal activity.
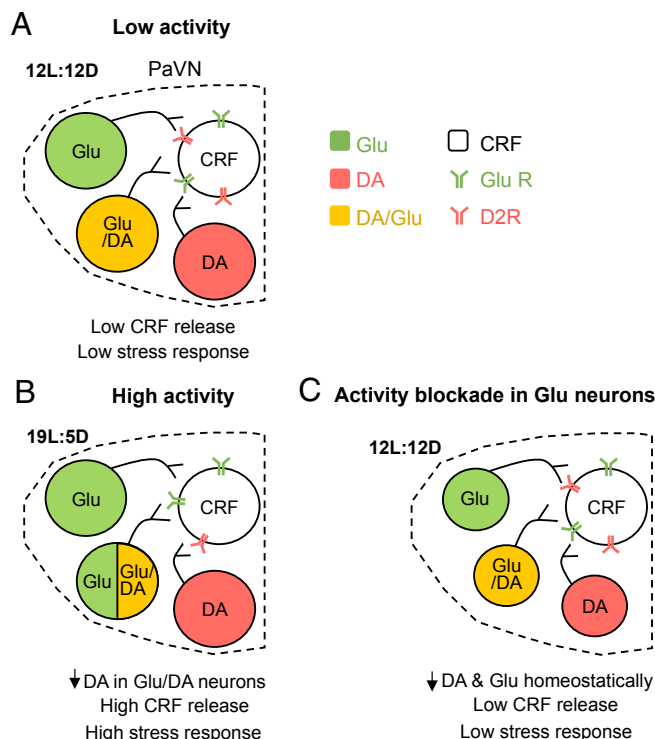
**Fig. 5.** Model of activity-dependent control of transmitter switching in the adult rat PaVN producing light-induced stress. (*A*) During the balanced-day photoperiod, the low activity of PaVN glutamatergic (Glu) neurons and inhibitory dopaminergic (DA) neurons leads to low activation of PaVN CRF neurons and a low stress response. (*B*) The shift to long-day photoperiod increases activation of PaVN Glu and DA neurons. Some Glu/DA neurons lose DA expression, while the level of Glu expression is maintained. Combined with the decreased CRF D2R level, CRF neurons are strongly activated and a high stress response is induced. (*C*) When the activity of PaVN Glu neurons is artificially suppressed, PaVN DA neurons down-regulate DA expression homeostatically. Whether both switching and nonswitching neurons target the same CRF cells remains to be determined.

## Materials and Methods

**Experimental Model and Subject Details.** All animal procedures were performed in accordance with institutional guidelines and approved by the University of California, San Diego Institutional Animal Care and Use Committee. Female TH-Cre Long–Evans rats, LE-Tg(TH-Cre)3.1Dei, were generously provided by Karl Deisseroth, Stanford University, Stanford, CA. The rat colony was maintained by breeding heterozygous female TH-Cre rats with male wild-type Long–Evans rats from a commercial source (Crl:LE; Charles River Laboratories). The offspring were genotyped using the following primers: Cre-forward AAGAACCTGATGGA-CATGTTCAGGGATCG and Cre-reverse CCACCGTCAGTACGTGAGATATCTTTAACC (19). Eight-week-old male TH-Cre offspring and their wild-type littermates were used in the study. Rats were group-housed, with food and water ad libitum, on a standard 12L:12D schedule (lights on at 7:00 AM) before any experimental procedures. For balanced-day (12L:12D) and long-day (19L:5D) photoperiod exposures, animals were housed singly in custom-made photo chambers for the indicated amount of time.

**Virus Injection.** Eight-week-old male rats were anesthetized with isoflurane during virus injection using a stereotaxic apparatus (David Kopf Instruments) and Hamilton syringe (no. 7647-1) and needle (33-gauge, no. 7762-06). The anterior PaVN (bregma: anteroposterior, −0.8; mediolateral, +0.8; dorso-ventral, −7.2, −7.0) was targeted, and a total of 1 μL of viral vector was injected into the PaVN unilaterally. The needle was left in place for 5 min after each injection. Serial dilutions of viral vectors were tested in WT and TH-Cre rats, and the lowest titers with a >50% infection rate after 4 wk were chosen for experiments. The vendors and final physical titers of viral vectors are as follows: AAVdj-CMV-DIO-Kir2.1-zsGreen, 3–5 × 10^13 genome copies (GC) per milliliter (GVVC-AAV-61; Stanford University Virus Core); AAVdj-EF1a-DIO-EYFP, 6–10 × 10^12 GC per milliliter (Karl Deisseroth; GVVC-AAV-13);

AAV1-hSyn-Cre-WPRE-hGH, 2.5 × 10^12 GC per milliliter (CS0646; Penn Vector Core); and AAV9-CaMKII0.4-Cre-SV40, 1.8 × 10^13 GC per milliliter (CS0569-3CS; Penn Vector Core).

**Immunofluorescent Staining.** At 10:00 AM–1:00 PM during the light cycle, rats were deeply anesthetized with pentobarbital sodium and perfused trans-cardially with 200 mL of 1× PBS, followed by 200 mL of 4% para-formaldehyde (PFA) in 1× PBS. Brains were then removed and postfixed in 4% PFA in 1× PBS at 4 °C overnight, followed by 30% sucrose for 4–5 d at 4 °C until the brains sank. Coronal sections (40 μm) were cut with a micro-tome and were ~20 μm postprocessing; every third section of the anterior PaVN was used for staining. Sections were incubated with a blocking solution (5% horse serum or 2% BSA in 1× PBS with 0.3% Triton X-100) for 2 h at room temperature (RT, 22 °C), and then incubated at 4 °C in the blocking solution with primary antibodies overnight. After rinsing in 1× PBS three times, for 10 min each time, sections were incubated in the blocking solution with secondary antibodies at RT for 2 h. Sections were then rinsed, mounted on glass slides with 2% gelatin, and coverslipped using Fluoromount-G (Southern Biotech) or ProLong Gold Antifade Mountant (Life Technologies). Five sections were examined per animal.

We used the following primary antibodies: mouse anti-TH (MAB318; Millipore), 1:200; rabbit anti-TH (AB152; Millipore), 1:500; mouse anti-VGLUT2 (MAB5504; Millipore), 1:100; goat anti–c-Fos (SC-52-G; Santa Cruz Biotechnology), 1:250; rabbit anti-nNOS (61-7000; Life Technologies), 1:500; mouse anti-NeuN (MAB377; Millipore), 1:500; and guinea pig anti-GFP (132 005; Synaptic Systems), 1:4,000. We used the following Alexa Fluor IgG secondary antibodies: 488 donkey anti-guinea pig, 488 donkey anti-rabbit, 555 donkey anti-Goat, 555 donkey anti-rabbit, and 647 donkey anti-mouse (all at 1:300; Life Technologies or Jackson ImmunoResearch).

**RNAscope in Situ Hybridization.** We used an RNAscope Multiplex Fluorescent Reagent Kit and Target Probes (Advanced Cell Diagnostics) for rat high-resolution in situ hybridization of TH mRNA and rat VGLUT2 (Slc17a6) mRNA. The experiment was performed according to the manufacturer's instructions. In an RNase-free environment, 16-μm fixed brain slices were sectioned and mounted on a glass slide immediately after microtome sectioning and baked in a 60 °C dry oven for 30 min; sections were ~8 μm postprocessing. Sections were rehydrated in PBS for 5 min before a 5-min incubation in 1× target retrieval solution at 90–95 °C. Sections were then rinsed with distilled water and 100% EtOH. Subsequently, sections were incubated with the following solutions in the HybEZ humidified oven at 40 °C with rinsing steps in be-tween: protease III, 30 min; target probes, 2 h; amplification (Amp) 1-fluo-rescence (FL), 30 min; Amp 2-FL, 15 min; Amp 3-FL, 30 min; and Amp 4-FL, 15 min. Amp 1-FL, Amp 2-FL, Amp 3-FL, and Amp 4-FL are all reagents included in the RNAscope Multiplex Fluorescent Reagent kit. Afterward, standard im-munofluorescent staining was performed using rabbit anti-TH (1:500) to de-tect TH protein in the same sections. Six sections were examined per animal.

**Confocal Imaging.** A Leica SP5 confocal microscope with a 25×/0.95 water-immersion objective was used to acquire all fluorescent images. The z-axis resolution of confocal images was 1.5 μm. For immunostained sections, a z-step of 1.5 μm was used to acquire the confocal images, resulting in 12–13 sections per stack. For cell counting, individual sections within the confocal stacks were examined, without maximal projection. Example images are maximum intensity projections of five sections of the confocal stack since maximal projection of the full stack resulted in many overlapping cells. For RNAscope, a z-step of 1 μm was used to acquire the confocal images, resulting in eight sections per stack. Example images are maximal projections of all eight sections of the confocal stack.

**TUNEL Assay.** We used an In Situ Cell Death Detection (TUNEL) Kit with TMR Red (12156792910; Roche) to detect apoptosis. PFA-fixed brain sections were mounted and dried on glass slides. After rehydration in 1× PBS for 5 min, sections were refixed with 1% PFA for 20 min at RT before rinsing in 1× PBS three times, for 5 min each time. Sections were then incubated in freshly prepared permeabilization solution (0.1% sodium citrate and 1% Triton X-100) for 1 h at RT. After rinsing, sections were incubated with TUNEL reaction mixture (250 μL per section, 25 μL of terminal-deoxynucleotidyl transferase solution + 225 μL of label solution) in a humidified chamber for 3 h at 37 °C in the dark. The sections were rinsed and mounted with DRAQ5-Fluoromount (1:1,000 dilution of DRAQ5 in Fluoromount-G). The positive control was treated with DNase I (10 U/mL, M0303S; New England Biolabs) for 1 h at 37 °C before the TUNEL reaction.

**Cell Number and Cell Density Quantification.** For c-Fos, TH, nNOS, TUNEL, and DRAQ5 quantification, individual sections within the 3D fluorescent confocal image stacks without maximal projection were used to manually count the number of cell bodies using the Leica Application Suite X software. For NeuN number and density, 3D fluorescent confocal image stacks were quantified with ImageJ software using the 3D objects counter and area measurement functions. Only the virus-expressing side of the PaVN was counted for virus-injected animals, while both sides of the PaVN were counted for the rest of the animals.

**Statistics.** Statistical analyses of the data were performed using Prism 7 software for the number of animals for each experiment indicated in the figure legends. Means and SEMs were reported for all experiments. For comparisons between two groups, Welch's $t$ test was used for normally distributed data and the Mann–Whitney $U$ test was used for data not normally distributed. For comparisons of more than two groups, ANOVA was used for normally distributed data, followed by Bonferroni post hoc analysis corrected for multiple comparisons. For data that were not normally distributed, the nonparametric Kruskal–Wallis test was used, followed by Dunn's post hoc analysis corrected for multiple comparisons. Values were considered significantly different at $P < 0.05$.

1. Christoffel DJ, Golden SA, Russo SJ (2011) Structural and synaptic plasticity in stress-related disorders. *Rev Neurosci* 22:535–549.
2. Bains JS, Wamsteeker Cusulin JI, Inoue W (2015) Stress-related synaptic plasticity in the hypothalamus. *Nat Rev Neurosci* 16:377–388.
3. Dulcis D, Jamshidi P, Leutgeb S, Spitzer NC (2013) Neurotransmitter switching in the adult brain regulates behavior. *Science* 340:449–453.
4. Gu X, Spitzer NC (1995) Distinct aspects of neuronal differentiation encoded by frequency of spontaneous Ca2+ transients. *Nature* 375:784–787.
5. Guemez-Gamboa A, Xu L, Meng D, Spitzer NC (2014) Non-cell-autonomous mechanism of activity-dependent neurotransmitter switching. *Neuron* 82:1004–1016.
6. Borodinsky LN, et al. (2004) Activity-dependent homeostatic specification of transmitter expression in embryonic neurons. *Nature* 429:523–530.
7. Marek KW, Kurtz LM, Spitzer NC (2010) cJun integrates calcium activity and tlx3 expression to regulate neurotransmitter specification. *Nat Neurosci* 13:944–950.
8. Moore RY (1983) Organization and function of a central nervous system circadian oscillator: The suprachiasmatic hypothalamic nucleus. *Fed Proc* 42:2783–2789.
9. Moore RY, Speh JC, Card JP (1995) The retinohypothalamic tract originates from a distinct subset of retinal ganglion cells. *J Comp Neurol* 352:351–366.
10. Moore RY (1996) Entrainment pathways and the functional organization of the circadian system. *Prog Brain Res* 111:103–119.
11. Earnest DJ, Olschowka JA (1993) Circadian regulation of c-fos expression in the suprachiasmatic pacemaker by light. *J Biol Rhythms* 8(Suppl):S65–S71.
12. Kornhauser JM, Nelson DE, Mayo KE, Takahashi JS (1990) Photic and circadian regulation of c-fos gene expression in the hamster suprachiasmatic nucleus. *Neuron* 5:127–134.
13. Aronin N, Sagar SM, Sharp FR, Schwartz WJ (1990) Light regulates expression of a Fos-related protein in rat suprachiasmatic nuclei. *Proc Natl Acad Sci USA* 87:5959–5962.
14. Munch IC, Møller M, Larsen PJ, Vrang N (2002) Light-induced c-Fos expression in suprachiasmatic nuclei neurons targeting the paraventricular nucleus of the hamster hypothalamus: Phase dependence and immunochemical identification. *J Comp Neurol* 442:48–62.
15. Vrang N, Larsen PJ, Møller M, Mikkelsen JD (1995) Topographical organization of the rat suprachiasmatic-paraventricular projection. *J Comp Neurol* 353:585–603.
16. Watts AG, Swanson LW, Sanchez-Watts G (1987) Efferent projections of the suprachiasmatic nucleus: I. Studies using anterograde transport of Phaseolus vulgaris leucoagglutinin in the rat. *J Comp Neurol* 258:204–229.
17. Buijs RM, Markman M, Nunes-Cardoso B, Hou YX, Shinn S (1993) Projections of the suprachiasmatic nucleus to stress-related areas in the rat hypothalamus: A light and electron microscopic study. *J Comp Neurol* 335:42–54.
18. Bullitt E (1990) Expression of c-fos-like protein as a marker for neuronal activity following noxious stimulation in the rat. *J Comp Neurol* 296:517–530.
19. Witten IB, et al. (2011) Recombinase-driver rat lines: Tools, techniques, and optogenetic application to dopamine-mediated reinforcement. *Neuron* 72:721–733.
20. Zhang S, et al. (2015) Dopaminergic and glutamatergic microdomains in a subset of rodent mesoaccumbens axons. *Nat Neurosci* 18:386–392.
21. Kubo Y, Baldwin TJ, Jan YN, Jan LY (1993) Primary structure and functional expression of a mouse inward rectifier potassium channel. *Nature* 362:127–133.
22. Hnasko TS, Edwards RH (2012) Neurotransmitter corelease: Mechanism and physiological role. *Annu Rev Physiol* 74:225–243.
23. Saunders A, Granger AJ, Sabatini BL (2015) Corelease of acetylcholine and GABA from cholinergic forebrain neurons. *eLife* 4:e06412.
24. O'Malley DM, Sandell JH, Masland RH (1992) Co-release of acetylcholine and GABA by the starburst amacrine cells. *J Neurosci* 12:1394–1408.
25. Gutiérrez R, et al. (2003) Plasticity of the GABAergic phenotype of the "glutamatergic" granule cells of the rat dentate gyrus. *J Neurosci* 23:5594–5598.
26. Simmons DM, Swanson LW (2009) Comparison of the spatial distribution of seven types of neuroendocrine neurons in the rat paraventricular nucleus: Toward a global 3D model. *J Comp Neurol* 516:423–441.
27. Hisano S, et al. (2000) Regional expression of a gene encoding a neuron-specific Na(+)-dependent inorganic phosphate cotransporter (DNPI) in the rat forebrain. *Brain Res Mol Brain Res* 83:34–43.
28. Fremeau RT, Jr, et al. (2001) The expression of vesicular glutamate transporters defines two classes of excitatory synapse. *Neuron* 31:247–260.
29. Aubry JM, Bartanusz V, Pagliusi S, Schulz P, Kiss JZ (1996) Expression of ionotropic glutamate receptor subunit mRNAs by paraventricular corticotropin-releasing factor (CRF) neurons. *Neurosci Lett* 205:95–98.
30. Spitzer NC (2017) Neurotransmitter switching in the developing and adult brain. *Annu Rev Neurosci* 40:1–19.
31. Dittgen T, et al. (2004) Lentivirus-based genetic manipulations of cortical neurons and their optical and electrophysiological monitoring in vivo. *Proc Natl Acad Sci USA* 101:18206–18211.
32. Bernstein HG, et al. (1998) Nitric oxide synthase-containing neurons in the human hypothalamus: Reduced number of immunoreactive cells in the paraventricular nucleus of depressive patients and schizophrenics. *Neuroscience* 83:867–875.
33. Gao SF, et al. (2014) Nitric oxide synthase and nitric oxide alterations in chronically stressed rats: A model for nitric oxide in major depressive disorder. *Psychoneuroendocrinology* 47:136–140.
34. Kishimoto J, Tsuchiya T, Emson PC, Nakayama Y (1996) Immobilization-induced stress activates neuronal nitric oxide synthase (nNOS) mRNA and protein in hypothalamic-pituitary-adrenal axis in rats. *Brain Res* 720:159–171.
35. Kügler S, Kilic E, Bähr M (2003) Human synapsin 1 gene promoter confers highly neuron-specific long-term transgene expression from an adenoviral vector in the adult rat brain depending on the transduced area. *Gene Ther* 10:337–347.
36. Roland BL, Sawchenko PE (1993) Local origins of some GABAergic projections to the paraventricular and supraoptic nuclei of the hypothalamus in the rat. *J Comp Neurol* 332:123–143.
37. Spitzer NC (2006) Electrical activity in early neuronal development. *Nature* 444:707–712.
38. Stuber GD, Stamatakis AM, Kantak PA (2015) Considerations when using cre-driver rodent lines for studying ventral tegmental area circuitry. *Neuron* 85:439–445.
39. Baker H (1990) Unilateral, neonatal olfactory deprivation alters tyrosine hydroxylase expression but not aromatic amino acid decarboxylase or GABA immunoreactivity. *Neuroscience* 36:761–771.
40. Kawano M, et al. (2006) Particular subpopulations of midbrain and hypothalamic dopamine neurons express vesicular glutamate transporter 2 in the rat brain. *J Comp Neurol* 498:581–592.
41. Sulzer D, et al. (1998) Dopamine neurons make glutamatergic synapses in vitro. *J Neurosci* 18:4588–4602.
42. Dal Bo G, et al. (2004) Dopamine neurons in culture express VGLUT2 explaining their capacity to release glutamate at synapses in addition to dopamine. *J Neurochem* 88:1398–1405.
43. Hnasko TS, et al. (2010) Vesicular glutamate transport promotes dopamine storage and glutamate corelease in vivo. *Neuron* 65:643–656.
44. Cole RL, Sawchenko PE (2002) Neurotransmitter regulation of cellular activation and neuropeptide gene expression in the paraventricular nucleus of the hypothalamus. *J Neurosci* 22:959–969.